

## Article

# Influence of Particle Size on Compressed Earth Blocks Properties and Strategies for Enhanced Performance

Chiara Turco <sup>1,2</sup>, Adilson Paula Junior <sup>1,2</sup> , Cláudia Jacinto <sup>1,2</sup>, Jorge Fernandes <sup>1,2</sup> , Elisabete Teixeira <sup>1,2</sup>   
and Ricardo Mateus <sup>1,2,\*</sup> 

<sup>1</sup> Department of Civil Engineering, University of Minho, 4800-058 Guimarães, Portugal; id9631@alunos.uminho.pt (C.T.); id8639@alunos.uminho.pt (A.P.J.); b13221@civil.uminho.pt (C.J.); jorge.fernandes@civil.uminho.pt (J.F.); elisabeteteixeira@civil.uminho.pt (E.T.)

<sup>2</sup> Institute for Sustainability and Innovation in Structural Engineering (ISISE), ARISE, University of Minho, 4800-058 Guimarães, Portugal

\* Correspondence: ricardomateus@civil.uminho.pt

**Abstract:** In the context of sustainable building development, Compressed Earth Blocks (CEBs) have garnered increasing attention in recent years owing to their minimal environmental and economic impact. However, owing to the inherent diversity of raw soil and the production process's reliance on expertise, the properties of these blocks are subjected to multifaceted influences. Among these, the significance of soil particle size variation often remains overlooked, leaving its impact ambiguous. This study endeavours to address this gap in existing research by delving into this aspect. Two distinct batches of CEBs were produced by adjusting the grain size curve of a single type of sieved soil with different maximum mesh openings: 2 mm for R1 CEBs and 12.5 mm for R2 CEBs. Experimental results reveal significant differences in thermophysical characteristics: on average, R1 blocks show superior thermal performance, boasting a 23% reduction in thermal conductivity compared to R2 blocks, and are lighter, with an 8% decrease in dry bulk density. Although no significant changes in mechanical parameters were observed, finer-structured R1 blocks showed a 25% greater tendency to absorb water due to changes in their porous structure. This study sheds light on the sensitivity of thermal parameters to changes in soil particle size and shows that blocks with finer particles exhibit poorer heat conduction and heat diffusion. Besides providing new insights into the literature, this research also provides a strategic approach to optimise the thermophysical properties of CEBs. By understanding the influence of particle size, researchers and practitioners can now develop strategies to enhance these properties and improve the overall performance of CEBs.

**Keywords:** particle size effect; soil texture; compressed earth blocks; thermophysical properties; mechanical properties; durability properties



**Citation:** Turco, C.; Paula Junior, A.; Jacinto, C.; Fernandes, J.; Teixeira, E.; Mateus, R. Influence of Particle Size on Compressed Earth Blocks Properties and Strategies for Enhanced Performance. *Appl. Sci.* **2024**, *14*, 1779. <https://doi.org/10.3390/app14051779>

Academic Editors: Daniel Ferrández Vega and Alexander Martín

Received: 23 January 2024

Revised: 14 February 2024

Accepted: 16 February 2024

Published: 22 February 2024



**Copyright:** © 2024 by the authors. Licensee MDPI, Basel, Switzerland. This article is an open access article distributed under the terms and conditions of the Creative Commons Attribution (CC BY) license (<https://creativecommons.org/licenses/by/4.0/>).

## 1. Introduction

In the context of the paradigm shift imposed by the climate crisis, the earth as a building material is gaining significant attention. It has proven to have a lower potential environmental impact with reduced CO<sub>2</sub> emissions [1] and decreased life cycle economic costs when compared to conventional building solutions. In addition to the environmental and economic benefits, the earth is an optimal candidate when it comes to energy efficiency due to its high thermal capacity that, if adequately combined with passive design strategies, including natural ventilation [2,3], can result in a comfortable indoor environment with very low energy consumption. Finally, its hygroscopic behaviour allows earthen structures to guarantee high levels of indoor air quality and healthfulness [4].

Compressed Earth Blocks (CEBs) are unfired masonry blocks made by mixing soil and water, a binder if necessary, and then compressed into blocks with a manual or hydraulic press. For this reason, they are considered the evolution of traditional adobe [5]. In modern applications, they could replace, for example, fired clay bricks or concrete blocks, the

production of which involves high energy consumption. However, modern applications require building materials to meet specific functional requirements. Despite the advantages listed above and the long tradition of earthen construction, many aspects related to the functional performance of these blocks are still unclear. This is especially the case with hygrothermal performance. In fact, while the numerous studies on mechanical aspects make it possible to affirm that the compressive strength of soil samples varies approximately between 1 and 2 MPa, the same cannot be said of thermo-hygro-metric parameters [6]. The data available in this area are much less and more scattered. Although an inverse linear correlation with bulk density is attributed to the thermal response [7], this has not yet been established with a reasonable degree of certainty. Indeed, it depends on many factors and the inherent variability of soils in nature, combined with the lack of experimental data, makes their characteristics unpredictable.

When evaluating the performance of the material, the influence of particle size is an aspect that is often overlooked [8]. Some studies addressed this aspect in compacted earth-based materials (e.g., hyper-compacted earth [8,9] or cement-stabilised soil cylinders [10]), but they tend to focus on (hygro-) mechanical or durability aspects. Such investigations reveal that finer-textured soils exhibit superior strength and durability than coarser soils. However, there is a gap in evaluating thermophysical attributes such as thermal conductivity and thermal capacity. Understanding these properties is crucial for assessing and optimising energy efficiency and overall thermal performance at the building scale. To the authors' best knowledge, there is only a study from 2019 [11] involving cement-stabilised rammed earth walls that found that grading differences can bring variations in the R-value. To study these grading differences, the authors of this research created a range of three subsoils by mixing a selection of gravel, sand, and silty clay in different proportions. The problem under consideration is also particularly interesting from a practical point of view. When it comes to earth as a building material, the natural soil grain distribution is often amended to obtain new, well-graded soil with desired characteristics. This is to guarantee the homogeneity of the mixture, which is essential to ensure a good porosity and porous structure, as well as stability. The addition of sand is the most common example, as it allows for better water permeability in the case of clayey soils [8,9]. On the contrary, sandy soils may lack cohesion and be weak or unstable [12]. In these cases, the addition of mineral stabilisers (lime or cement) is common [13]. Alternatively, soils can be collected from various sites [10]. Other less conventional approaches found in the literature are (i) the addition of lime-cement blend [13], (ii) the reduction of clay and silt content via washing [14], and (iii) the addition of a mix of river sand and construction and demolition waste [15]. These studies investigate the effect of grain size curve corrections on the quality of the newly obtained soils, mainly through mechanical and durability tests. However, these corrections bring microstructural, mineralogical and, more generally, physical changes, which inevitably interfere with the thermo-hygro-metric attributes.

#### *Aim of the Study*

This study aims to explore the influence of maximum soil particle size on the properties of CEBs. The blocks under investigation were produced by a company in southern Portugal that specialised in earthen construction. From the natural soil, two different batches of blocks were obtained by sieving it with different maximum mesh openings: 2 mm for R1 CEBs (fine texture) and 12.5 mm for R2 CEBs (coarse texture). The grain size curve corresponding to the first case (R1) conforms to the grain size curve recommended by CRAterre [16], while the second (R2) represents the gradation of the soil typically used by the company that produced the blocks. This approach allowed the variable under investigation to be isolated, avoiding the introduction of new variables due to the addition of different materials to correct the grain-size curve.

## 2. Materials and Methods

The manufacturing company supplied all the raw materials: soil, water, and hydraulic lime used for stabilisation. The soil was characterised in the laboratory, where all the main geotechnical and physical investigations were performed. The results of the characterisation are reported in the following section. No detailed analyses were performed on the other materials. However, the water used was tap water, and the hydraulic lime was a commercial product, NHL5 type.

### 2.1. Soil Characterisation

The characterisation of soil was performed through the main geotechnical and physical analyses: Particle Size Distribution (PSD), Atterberg limits, particle density, Optimum Water Content (OWC), sand equivalent test, blue methylene test and organic matter content. Differential Scanning Calorimetry (DSC) was used to estimate the specific heat.

The granulometric curve (Figure 1) shows a well-graded natural soil (black line) with an adequate clay content (~6.50%) for the production of CEBs. The only correction needed was related to the exclusion of the coarse gravel fraction (20–63 mm) [17]. The graph also shows the PSD curves of the two soils under investigation: (i) R1 Soil, with a maximum particle size  $\leq 2.0$  mm, and (ii) R2 Soil, with a maximum particle size  $\leq 12.5$  mm. Furthermore, the graph provides the upper and lower limits of particle size distribution recommended by CRATERre [16].

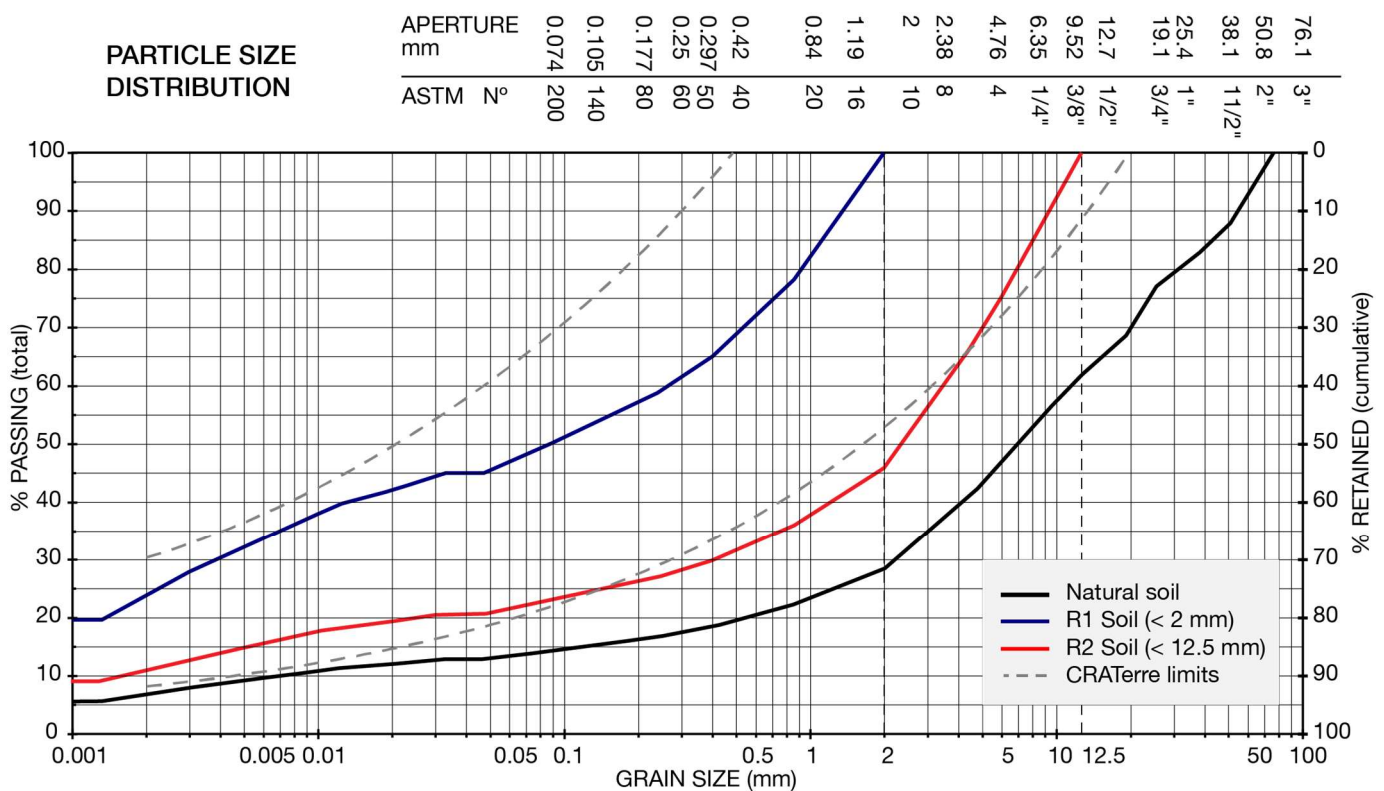


Figure 1. Particle size distribution curves.

Table 1 summarises soil characteristics, along with test methods and standard procedures followed.

**Table 1.** Physical and geotechnical characteristics of the soil used.

	R1 Soil ( $\leq 2.0$ mm)		R2 Soil ( $\leq 12.5$ mm)		Test Methods	Standards
Consistency limits <sup>1</sup>	$w_L = 29.5\%$ , $w_P = 18.5\%$ , $IP = 11\%$				Atterberg limits	NP-143 [18]
Particle density <sup>1</sup>	2.71 g/cm <sup>3</sup>				Pycnometer test	NP-83 [19]
Specific heat (at 26.85 °C) <sup>1,2</sup>	883.93 J/kg°C				Diff. Scan. Calorim.	ASTM E1269 [20]
Maximum dry density	1.97	g/cm <sup>3</sup>	2.01	g/cm <sup>3</sup>	Proctor test	E 197 (1966) [21]
Optimum water content	12.2	%	12.0	%		
Sand content	15.34	%	18.80	%	Sand equivalent test	NP EN933-8 (2002) [22]
Activity of clay minerals	0.57	mg/g	0.67	mg/g	Blue methylene test	NP EN933-9 (2002) [23]
Organic content	3.90	%	3.50	%	Loss on ignition test	ASTM D2974 [24]

<sup>1</sup> This test was performed only once for both soils as it is standardised for a maximum particle size equal to 4.75 mm. <sup>2</sup> Due to the apparatus's calibration, it was impossible to get reliable measurements at 20 °C.

Based on these results, both soils can be classified as “sandy and silty” [25]. The Atterberg limits fall within the range recommended by the well-known review article by Delgado and Guerrero [17], i.e., 25–51% for the liquid limit ( $w_L$ ) and 2–31% for the plasticity index (IP). From a geotechnical and physical point of view, the soils obtained—also considering the mild stabilisation with hydraulic lime—are suitable for CEB production. The appearance of the two derived soils is reported in Figure 2.



**Figure 2.** (a) Appearance of R1 soil (maximum particle size < 2 mm), and (b) appearance of R2 soil (maximum particle size < 12.5 mm).

## 2.2. Compressed Earth Blocks Production and Curing

The two soils were used to produce different batches of blocks: (i) fine-textured R1 CEBs (<2 mm) and coarse-textured R2 CEBs (<12.5 mm). Both batches underwent an identical production process. The mixtures were designed on a volumetric basis. The mixing process was executed manually, combining soil, water, and 5% volume of hydraulic lime for stabilisation. Initially, soil and lime were mixed dry to ensure a uniform distribution of the stabiliser. Water was gradually added until the desired consistency specified by the manufacturer was achieved. The resulting mixture was then placed in a single ram hydraulic press (Eco Máquinas, São Domingos, Brazil—Eco Master 7000 Turbo II) to create blocks with standard dimensions of 300 mm × 150 mm × 80 mm (Figure 3). Please note that the blocks may vary in thickness by  $\pm 7$  mm.

The produced blocks were subsequently stored in a sheltered area, covered with plastic sheets, and left to air dry. During the first week, they were hydrated twice a day to aid the maturation process. The blocks were tested at the age of 28 and 180 days.



**Figure 3.** Freshly compressed earth blocks (R1 type).

### 2.3. Compressed Earth Blocks Characterisation

This study employs a comprehensive array of testing methods, including both destructive and non-destructive approaches, alongside analytical formulations, to thoroughly characterise the main physical, thermal, mechanical and durability properties of the blocks. Each test was conducted on three CEBs. The 180-day compression tests were instead conducted on six blocks. Thirty-six samples were analysed from each batch of CEBs (R1 and R2), eighteen of each age, resulting in a total of seventy-two blocks examined.

#### 2.3.1. Bulk Density, Open Porosity, and Moisture Content

All the blocks were characterised geometrically, and their mass was measured at their natural moisture content. The bulk density  $\gamma$  was then measured using Equation (1), Table 2. Blocks were kept at the same temperature and humidity conditions throughout the experimental campaign. The dry bulk density  $\gamma_d$  was obtained by measuring the dry mass of blocks dried in an oven at  $40 \pm 5$  °C to a constant mass. From here, the open porosity  $\varphi$  and moisture content  $\omega$  were estimated according to Equations (2) and (3).

**Table 2.** Physical attributes considered.

Characteristics	Equations	Units	Symbols
Bulk density	$\gamma = m/V$ (1)	[kg/m <sup>3</sup> ]	$m$ and $V$ are the mass and the volume of the block
Open porosity	$\varphi = 1 - (\gamma_d/\gamma_s)$ (2)	[%]	$\gamma_d$ is the dry bulk density, $\gamma_s$ and is the soil particle density (Table 1)
Natural moisture content	$\omega = (\gamma - \gamma_d)/\gamma$ (3)	[%]	$\gamma$ is the bulk density at the natural moisture content, $\gamma_d$ is the dry bulk density

#### 2.3.2. Thermal Resistance, Conductivity, and Diffusivity

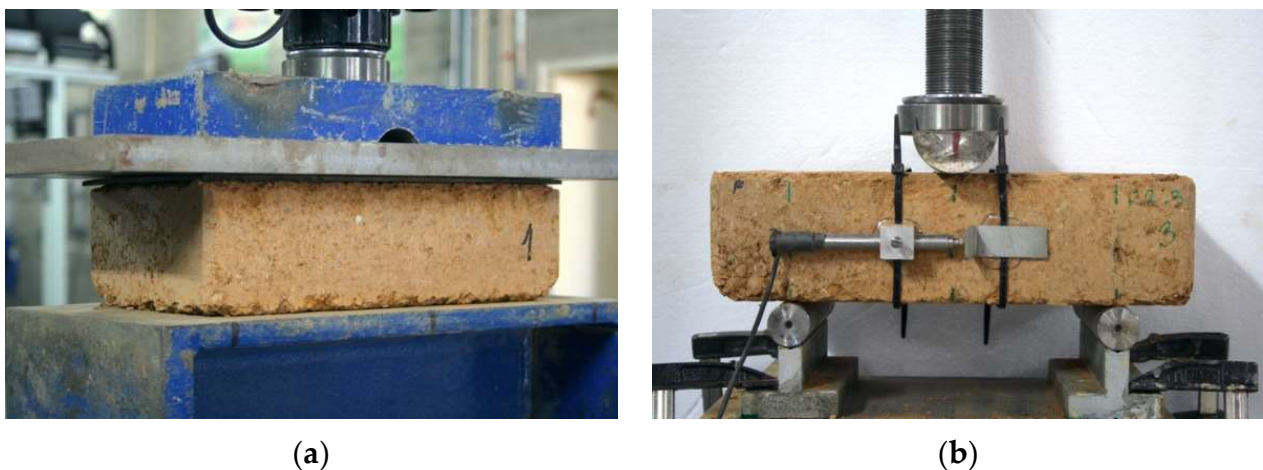
The thermal resistance was measured under steady-state conditions using the guarded hot box method, according to ASTM C1363-11:2011 [26] and ISO 9869-1:2014 [27]. Each block was placed between two sensors in a temperature-controlled enclosure, while a known temperature difference was applied between the two block faces. The sensors measured the heat flux passing through, and the R-value is estimated through Equation (4), Table 3. Steady-state conditions are assumed to be verified when the percentage change in heat flux throughout the sample is  $\leq 5\%$  at 24-h intervals and after a minimum of 72 h of testing. A more detailed description of the test setup and method can be found in [28]. Thermal conductivity and diffusivity were then deduced analytically according to Equations (5) and (6).

**Table 3.** Thermal attributes considered.

Characteristics	Equations	Units	Symbols
Thermal resistance	$R = \Delta T/q$ (4)	[m <sup>2</sup> K/W]	$\Delta T$ is the temperature difference, and $q$ is the heat flux
Thermal conductivity	$\lambda = d/R$ (5)	[W/mK]	$d$ is the thickness of the material, and $R$ is the thermal resistance
Thermal diffusivity	$\alpha = \lambda/(\gamma C_p)$ (6)	[m <sup>2</sup> /s]	$\lambda$ is the dry-state thermal conductivity, $\gamma$ is the bulk density, and $C_p$ is the specific heat (see Table 1)

### 2.3.3. Compressive Strength, E-Modulus and UPV

The compressive strength was estimated through uniaxial and unconfined compression tests on the blocks, according to NP EN 772-1 [29]. A rubber sheet was placed to cover the surface of the block to mitigate possible friction with the load plate due to the difference in stiffness between the steel and the earth block. The blocks were tested in a flat position in displacement control at a speed of 0.5 mm/s (Figure 4a). The ultimate compressive strength was estimated through Equation (7), Table 4. The E-Modulus, or modulus of elasticity, was derived from the compression test as the ratio of stress to strain in the linear elastic region of the stress-strain curve (Equation (8)).

**Figure 4.** Mechanical tests: (a) compression test and (b) three-point bending test on R2 CEB specimen.**Table 4.** Mechanical attributes considered.

Characteristics	Equations	Units	Symbols
Ultimate compressive strength	$\sigma_c = F/A$ (7)	[MPa]	$F$ is the maximum load achieved before rupture, and $A$ is the contact area
E-Modulus	$E = \sigma/\epsilon$ (8)	[MPa]	$\sigma$ and $\epsilon$ are stress and strain of the elastic section
Ultrasound Pulse Velocity	$UPV = L/t$ (9)	[m/s]	$L$ is the distance between the transducers considered, and $t$ is the time
Ultimate flexural strength	$\sigma_f = 3FL/2bd^2$ (10)	[MPa]	$F$ is the maximum load achieved before rupture, $L$ is the support span, and $b$ and $d$ are the block's width and thickness, respectively

Prior to the compression test, the ultrasonic pulse velocity (UPV) test method was performed on selected blocks in accordance with NP EN 12504-4 [30]. This non-destructive method consists of measuring the time in which an ultrasonic pulse propagates in the medium under consideration (Equation (9)). The UPV was measured six times on each block to check whether there was a relationship between the physical and mechanical parameters considered. A Portable Ultrasonic Non-destructive Digital Indicating Tester

(Proceq PUNDIT Lab) was used. A coupling gel was used to ensure better contact between the surface of the blocks and the transducers. According to [31,32], 54 kHz was used as the appropriate emission frequency for earthen blocks.

### 2.3.4. Flexural Strength

The flexural strength was estimated through the three-point bending test (Figure 4b). The blocks were placed on two-point support with a 200 mm span. The load was applied to the centre of the upper surface in displacement control at 0.005 mm/s. The ultimate strength was then calculated as Equation (10), Table 4.

### 2.3.5. Water Absorption by Capillarity and Electrical Resistivity Test

The LNEC E 393 [33] procedure was adapted to measure the capillary water absorption. Oven-dried blocks were placed sideways in a plastic box with a thin layer of water ( $5 \pm 1$  mm). At specific time intervals, the change in weight and height (in centimetres) of the capillary rise of water was measured. The capillarity coefficients were estimated through Equation (11), Table 5. After the test, the electrical resistivity was measured on saturated blocks. This non-destructive test consists of passing an electrical current and measuring the resulting voltage drop. A ResipodProceq equipment was used in this study (Figure 5a). The electrical resistivity is calculated using Ohm’s law (Equation (12)).

**Table 5.** Durability attributes considered.

Characteristics	Equations	Units	Symbols
Water absorption by capillarity	$C_b = (m_1 - m_0)/A\sqrt{t}$ (11)	[g/(cm <sup>2</sup> √min)]	$m_0$ is the mass of the block before immersion in water, $m_1$ is the mass of the block after immersion in water, $A$ is the contact area, and $t$ is the immersion time
Electrical resistivity	$\rho = V/I$ (12)	[kΩcm]	$V$ is the voltage, and $I$ is the current
Water absorption by total immersion	$W = (m_1 - m_0)/(m_1 - m_2)$ (13)	[%]	$m_0$ is the dry mass of the specimen, $m_1$ is the saturated mass of the specimen in the air, and $m_2$ is the hydrostatic mass of the saturated specimen
Erodibility index	$D = d/t$ (14)	[mm/hr]	$d$ is the thickness of the block, and $t$ is the time taken for full penetration

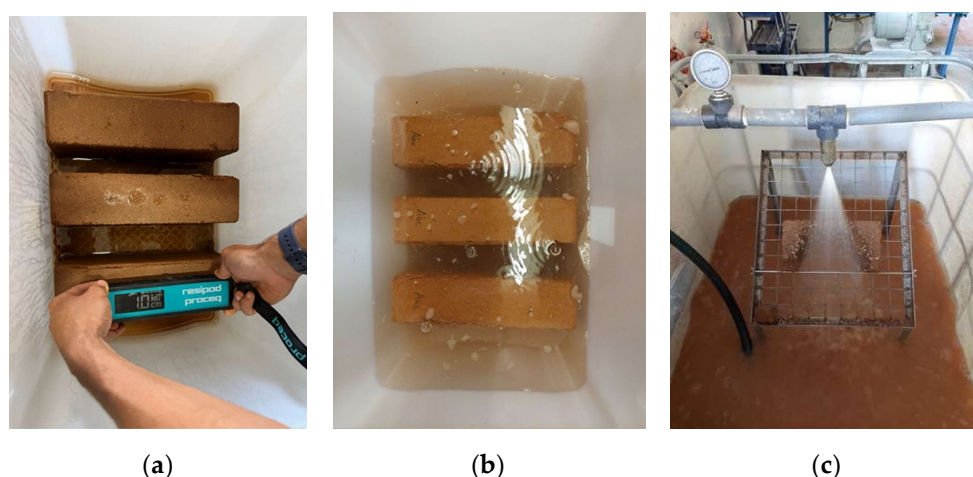


**Figure 5.** Durability tests: (a) CEBs after saturation during electrical resistivity measurement, (b) total water immersion and (c) erosion test setup.

### 2.3.6. Water Absorption by Total Immersion

The total water absorption by immersion was measured by adapting from LNEC E 394 [34]. The oven-dried blocks were placed in a plastic box and immersed in water at

$20 \pm 3$  °C (Figure 5b). The mass change was measured at regular intervals, and the percentage of absorption was calculated according to Equation (13), Table 5.

### 2.3.7. Erodibility Index

The erodibility index was assessed through the accelerated erosion test, or pressure spray method, according to NZS 4298 [35]. The test consists of spraying high-pressure water (45 kPa) on the upper face of the specimen placed on a support with an inclination of  $30^\circ$ . The test lasts one hour or until the block is penetrated (Figure 5c). The depth of erosion calculated according to Equation (14), Table 5, is the criterion for defining the erodibility index on a scale from 1 to 5, from a slightly erodible sample to a disintegrated sample.

## 3. Results and Discussion

### 3.1. Bulk Density, Open Porosity, and Natural Moisture Content

The bulk density of R1 blocks is lower than that of R2 blocks, on average 8%. The former are in the  $1650\text{--}1800$   $\text{kg}/\text{m}^3$  range, while the latter are in the  $1800\text{--}1950$   $\text{kg}/\text{m}^3$  range, as shown in Figure 6. Note the presence of two possible outliers around  $2000$   $\text{kg}/\text{m}^3$ .

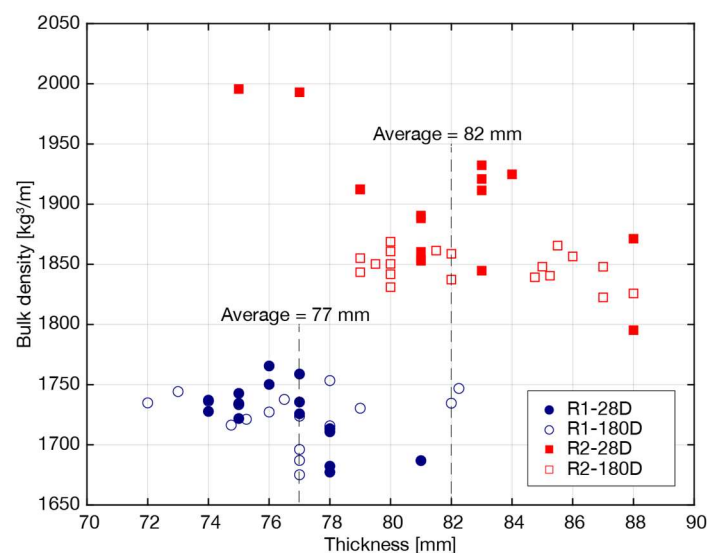


**Figure 6.** Differences in thickness and bulk density due to particle size effect.

In general, fine-grained soils allow for a closer arrangement of particles when subjected to the same degree of compression. This greater compaction capacity is evident when examining the thickness of R1 blocks ( $77 \pm 2.25$  mm), which is systematically lower than that of R2 blocks ( $82 \pm 3.36$  mm). On the other hand, a more packed structure has reduced void spaces, resulting in a denser configuration [36,37]. The results of this study do not support this theory despite the fact that soil R1 has a heavier, fine-grained fraction than soil R2. Possibly, in the soil under investigation, the removal of particles larger than 2 mm resulted in the removal of a group of coarser, heavier particles and the reconfiguration of the granule-porous structure [38].

Open porosity was estimated at 36% for R1 blocks and 32% for R2 blocks. Therefore, the less dense blocks are also more porous (this result was further confirmed by the results of water absorption and electrical resistivity presented later).

The natural moisture content was different at 28 and 180 days. At 28 days, both mixtures showed an average moisture content of 1.40%, with a high coefficient of variations (45%). At 180 days, typical values were 0.80% for R1 CEBs and 0.60% for R2 CEBs. The latter values fall within the common range of humidity (0.50 to 5% [39]). The higher moisture content detected in R1 blocks was expected, as finer particles tend to retain water more easily than coarser ones [40].

### 3.2. Thermal Resistance, Conductivity, and Diffusivity

From the point of view of a building material, experimental results show that finer-grained blocks (R1) exhibited better thermal performance than coarser-grained blocks (R2). R1 CEBs showed a 30% increase in thermal resistance compared to R2 CEBs due to the sole effect of different maximum particle sizes. A substantial reduction in thermal conductivity and diffusivity, by 23% and 17% respectively, is noticeable. Table 6 summarises the results obtained per mixture and age.

**Table 6.** Thermal attributes of R1 (finer-grained) and R2 (coarser-grained) CEBs <sup>1</sup>.

	R1 CEBs				R2 CEBs			
	$\gamma_d$ [kg/m <sup>3</sup> ]	R-Value [m <sup>2</sup> K/W]	$\lambda$ [W/mK]	$\alpha$ [m <sup>2</sup> /s]	$\gamma_d$ [kg/m <sup>3</sup> ]	R-Value [m <sup>2</sup> K/W]	$\lambda$ [W/mK]	$\alpha$ [m <sup>2</sup> /s]
28 days	1682.16 ± 4.78 (0.28%)	0.302 ± 0.023 (7.65%)	0.501 ± 0.039 (7.72%)	$3.37 \times 10^{-7}$ ± 2.52 × 10 <sup>-8</sup> (7.46%)	1830.98 ± 31.21 (1.70%)	0.232 ± 0.010 (4.31%)	0.653 ± 0.030 (4.66%)	$4.04 \times 10^{-7}$ ± 2.56 × 10 <sup>-8</sup> (6.33%)
180 days	1733.67 ± 15.64 (0.90%)	0.299 ± 0.026 (8.55%)	0.505 ± 0.045 (8.90%)	$3.29 \times 10^{-7}$ ± 2.76 × 10 <sup>-8</sup> (8.37%)	1842.59 ± 4.75 (0.26%)	0.231 ± 0.010 (4.13%)	0.650 ± 0.027 (4.11%)	$3.99 \times 10^{-7}$ ± 1.72 × 10 <sup>-8</sup> (4.32%)

<sup>1</sup> This table shows the average data with its standard deviation and, in brackets, the coefficient of variation.

The results suggest that the size of the maximum soil particles can significantly influence the thermophysical properties of CEBs. To study the problem and isolate the considered variable, other important factors were kept constant. These are:

- Soil particle mineralogy—the sieving strategy adopted to modify the grain size curve of the natural soil made it possible not to alter its mineralogy. Alternatively, sand should have been added. Considering that quartz, the most common constituent of sand can have three times higher the thermal conductivity of clay minerals, i.e., 8.80 W/mK vs. 3.0 W/mK [41], it is reasonable to suspect that, when this element is added to alter the PSD of the soil, the thermal response will inevitably be altered as well.
- Degree of compaction—the applied pressure can significantly affect particle packing and the overall heat and mass transfer mechanisms [9,42,43]. In this study, the degree of compaction was kept constant as the blocks underwent the exact same manufacturing process.
- Moisture content—thermal results presented refer to a dry-reached state. It is generally acknowledged that moisture content has a great influence on the thermal attributes of a hygroscopic material such as soil. However, the extent of this influence has not been conclusively established [4]. Consequently, when presenting thermal parameters, it is common to refer to dry-state conditions to avoid excessive fluctuations in results and to establish a baseline. Indeed, depending on the degree of saturation, water menisci between soil particles act as bridges for heat transfer. A study from 2015 [38] showed that thermal conductivity was lower in fine sands than in coarse ones under dry conditions but higher in fine sands than in coarser ones at low moisture content.

Considering the above, the increase in thermal resistance can be attributed to finer particles in R1 CEBs. This resistance is due to the more numerous contact zones between smaller grains, which, when filled with air, offer greater resistance to heat flow [38,44]. In fact, finer particles make the surface area of a given portion of material larger than the same portion composed of coarser particles. In the former case, the contact areas increase, and the heat flow encounters more dispersion points. The mechanism is presented in Figure 7.

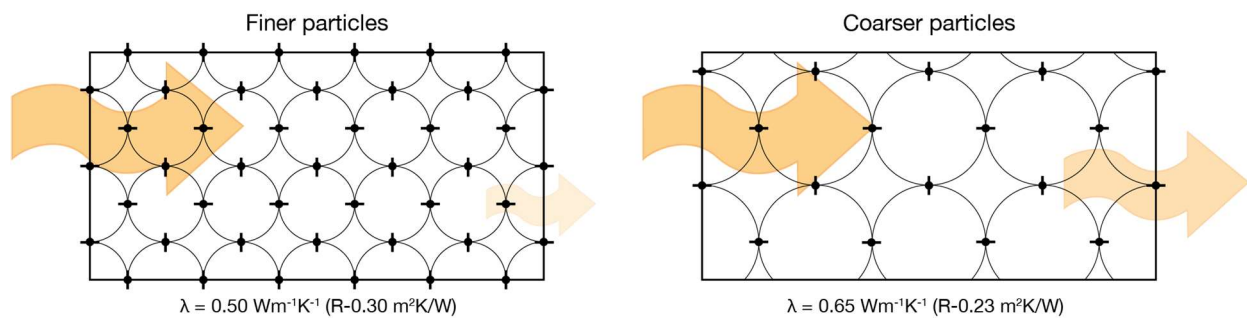


**Figure 7.** Simplified heat transfer mechanism in dry conditions: finer-grained soils (**left**) have a greater surface area than coarser-grained soils (**right**). In the former case, the more contact points dampen the heat flow to a greater extent.

The estimated thermal characteristics fall within the intervals reported in the literature. Thermal conductivity values for unfired stabilised CEBs generally range between 0.40 and 1.20 W/mK, heat capacity between 870 and 1180 J/kgK, and thermal diffusivity between  $3.02 \times 10^{-7}$  and  $4.82 \times 10^{-7}$  m<sup>2</sup>/s [39,45]. Consistent with previous studies on earth-based building materials [7,46–50], the observed trend is a decrease in thermal conductivity in blocks with lower bulk density (Figure 8).

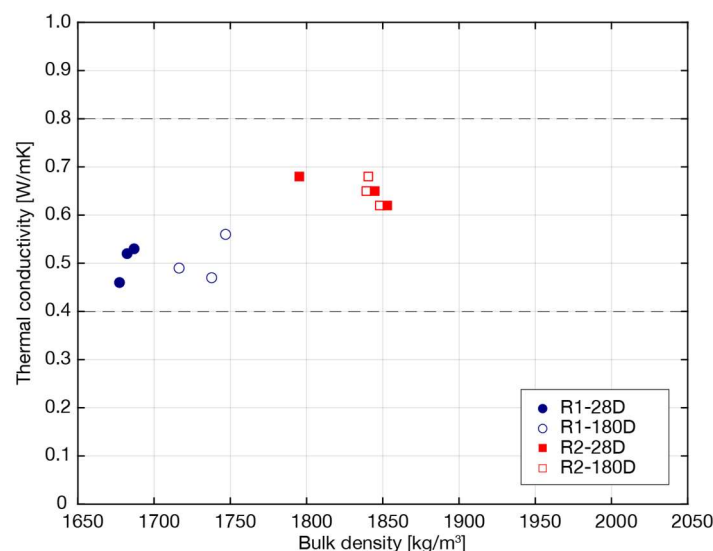


**Figure 8.** Bulk density vs. thermal conductivity of the two batches of CEBs at both ages.

It can be stated that less dense blocks generally have a higher porosity. In dry conditions, air-filled porosity reduces the thermal conductivity of the blocks due to the inherently low thermal conductivity of air. Therefore, dry density and porosity considerably affect dry soils' conductivity, as heat transfer only depends on the physical contact between the soil particles [38]. Although, in this case, one can refer to an inverse linear relationship, as soon as an increase in humidity is considered, thermal conductivity increases in a non-purely linear trend [41].

Neglecting the water component may have led to an underestimation of the results. The evaluation of effective thermal parameters is still a challenge in soil science. Considering the discussion presented so far, future studies will be focused on modelling the effective thermal parameters of blocks and conducting parametric analyses on wall systems, considering the standard variations in the moisture content.

### 3.3. Compressive Strength, E-Modulus and UPV

Table 7 shows the results obtained from the compression tests performed directly on blocks. Unlike more conventional cubic or cylindrical samples, this is a common practice in CEBs, notwithstanding the lack of standardised aspect ratio correction factors, and this leads to an effective strength overestimation [51]. The displacement control has been chosen instead for better control of the failure pattern.

**Table 7.** Compression test and UPV test results <sup>1</sup>.

	R1 CEBs				R2 CEBs			
	$\gamma$ [kg/m <sup>3</sup> ]	$\sigma_c$ [MPa]	E-Modulus [MPa]	UPV [m/s]	$\gamma$ [kg/m <sup>3</sup> ]	$\sigma_c$ [MPa]	E-Modulus [MPa]	UPV [m/s]
28 days	1720.47 ± 14.50 (0.84%)	2.54 ± 0.33 (13.01%)	55.65 ± 21.22 (38.13%)	1018.65 ± 104.83 (10.29%)	1945.79 ± 42.05 (2.16%)	2.27 ± 0.34 (15.00%)	53.61 ± 1.69 (3.15%)	1004.57 ± 87.21 (8.68%)
180 days	1727.49 ± 15.47 (0.90%)	1.78 ± 0.11 (6.42%)	40.46 ± 2.12 (5.25%)	974.71 ± 28.15 (2.89%)	1848.36 ± 10.66 (0.58%)	2.03 ± 0.23 (11.49%)	46.21 ± 1.86 (4.02%)	1113.33 ± 63.46 (5.70%)

<sup>1</sup> This table shows the average data with its standard deviation and, in brackets, the coefficient of variation.

From the results obtained, the expected linear relationship between bulk density and compressive strength was not found [7]. Nevertheless, compressive strength values align in an almost constant range (1.5–3 MPa), as shown in Figure 9a. The elastic modulus indicates that both batches of blocks are stiffer at 180 days. As for the UPV test results, Figure 9b shows the data collected.

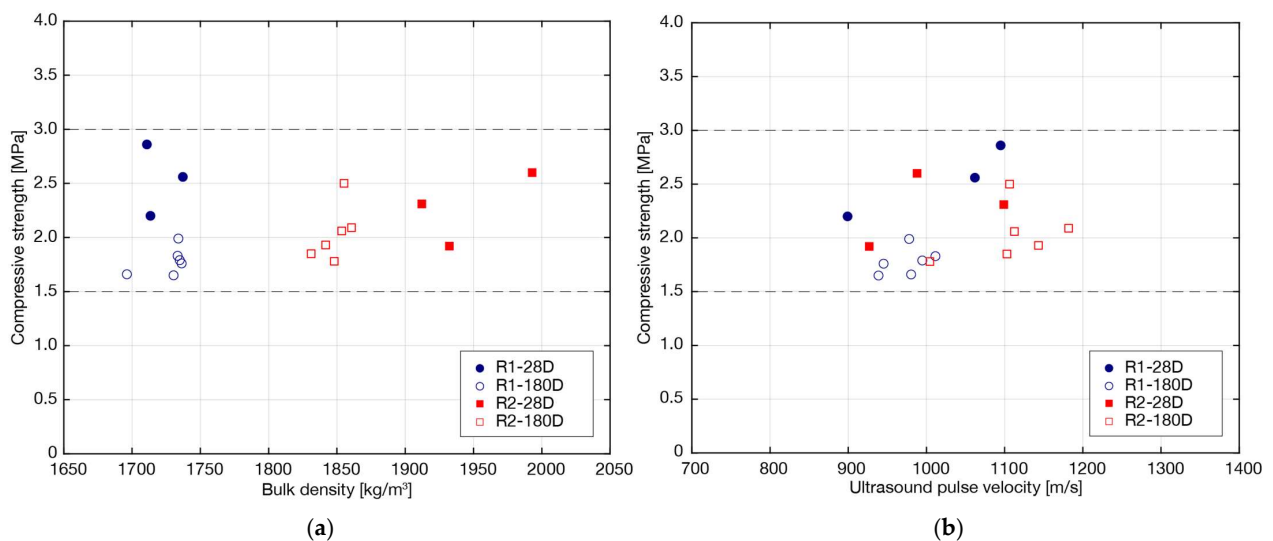


**Figure 9.** (a) Bulk density vs. compressive strength; (b) Bulk density vs. UPV.

Interestingly, the data show that the compressive strength of both batches of blocks decreases slightly from 28 to 180 days, especially in finer-textured R1 CEBs. In fact, at 180 days, R1 CEBs exhibit 30% lower strength than at 28 days, and CEB R2 is 11% lower. It should be noted that the coefficients of variation of the 28-day results are higher than those at 180 days. Moreover, the values do not show a well-defined trend. This result could, therefore, be attributed to a mere dispersion in the data. However, specific studies need to be carried out to ascertain whether this was an actual degradation of bond strengths, especially in the finer-grained CEBs, and the reasons behind it.

Concerning the results of the UPV test, in both mixtures, at 28 days, the results were not indicative. They fell in the same range and were practically superimposable. At 180 days,

however, the propagation speed was higher in R2 blocks (denser, less porous, but also less humid) and lower in R1 blocks (less dense, more porous, and more humid), as predicted by theory (in theory, the ultrasonic pulse should propagate faster in denser media. The pores, in fact, tend to obstruct the path of the wave). The results obtained could be attributed to the moisture content, which, let us recall, at 28 days in both batches was 1.40% and at 180 days in the R1 blocks was 0.80% and in the R2 blocks 0.60%. However, further studies are needed to confirm this hypothesis. To the best of the authors' knowledge, the few studies available on the subject have found a direct relationship between wave propagation speed and compressive strength [32,52,53]. According to this, faster waves correspond to denser and, in general, more resistant media. Idder et al. [54] refer to an inverse correlation between porosity and UPV, like the fact that as porosity increases, density decreases and with-it resistance. Teixeira et al. [28] agree with the common assumption that faster waves are related to denser blocks. However, it is difficult to place the results obtained in a broader, generalised context. Therefore, the sought-after correspondence between the mentioned properties was not found. Further studies and experimental data are certainly needed to verify this relationship and validate any correlations to bridge this gap.

### 3.4. Flexural Strength

Flexural strength is commonly used to measure tensile strength indirectly [55]. The use of this kind of test is important for two main reasons: (i) the setup is easy and quick to perform even in situ for block quality control; (ii) it provides insights for comparing simple mixtures with fibre-reinforced mixtures. Table 8 shows the experimental results obtained from the three-point bending test.

**Table 8.** Three-point bending test results <sup>1</sup>.

	R1 CEBs		R2 CEBs	
	$\gamma$ [kg/m <sup>3</sup> ]	$\sigma_f$ [MPa]	$\gamma$ [kg/m <sup>3</sup> ]	$\sigma_f$ [Mpa]
28 days	1737.45 ± 18.53 (1.07%)	0.25 ± 0.014 (5.59%)	1944.29 ± 44.92 (2.32%)	0.21 ± 0.008 (3.66%)
180 days	1730.14 ± 20.32 (1.17%)	0.25 ± 0.030 (11.92%)	1859.05 ± 7.92 (0.43%)	0.22 ± 0.019 (8.41%)

<sup>1</sup> This table shows the average data with its standard deviation and, in brackets, the coefficient of variation.

Less-dense R1 CEBs exhibited a slightly higher bending strength (Figure 10). However, the two parameters do not have a clear, direct relationship, and the difference between the two mixtures is not significant.

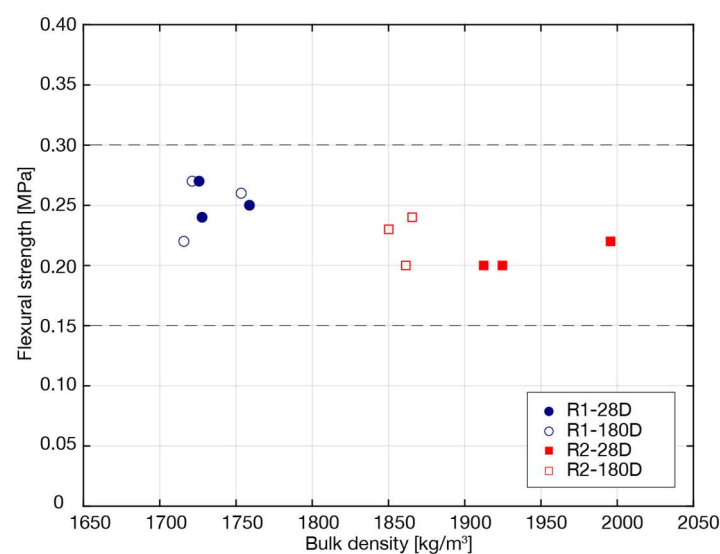


**Figure 10.** Bulk density vs. flexural strength.

### 3.5. Water Absorption by Capillarity and Electrical Resistivity

The grams of water absorbed by capillarity are proportional to the square root of time [45]. The graph in Figure 11 shows this relationship, averaging the results obtained in the three samples tested per mixture.

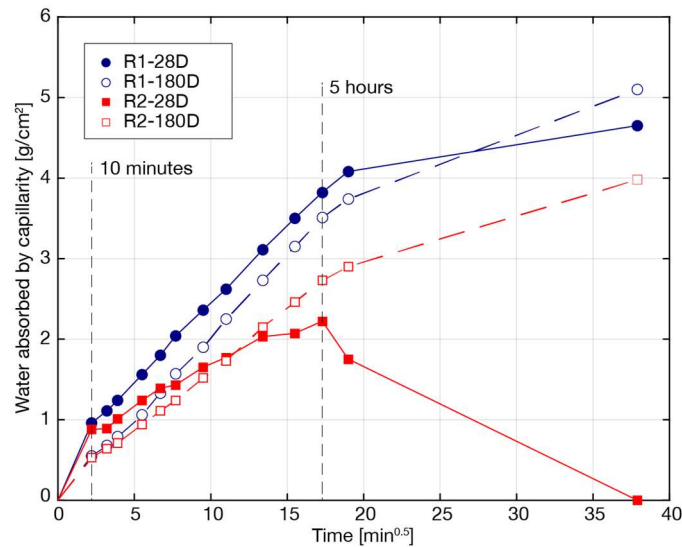


**Figure 11.** Evolution of the water absorbed per unit of surface area with the square root of time.

After 10 min, the water absorbed per unit area by the two mixtures is virtually identical. The greater slope of the initial section indicates that water absorption by capillarity is faster in the first few minutes [45]. Only later does it become less important, and a reduction in the slope curves can be observed. This is particularly evident in R2 CEBs, indicating their lower water absorption capacity. For a more immediate comparison, a single value can be obtained by considering the angular coefficient of the straight line passing between the capillarity coefficients at 10 min and 5 h [45]. This number, denoted as  $C_b$ , along with the dry bulk density ( $\gamma_d$ ) and the electrical resistivity ( $\rho$ ) measured at the end of the capillarity test on saturated blocks, is reported in Table 9.

**Table 9.** Water absorption by capillarity test results <sup>1</sup>.

	R1 CEBs			R2 CEBs		
	$\gamma_d$ [kg/m <sup>3</sup> ]	$C_b$ [g/(cm <sup>2</sup> √min)]	$\rho$ [kΩcm]	$\gamma_d$ [kg/m <sup>3</sup> ]	$C_b$ [g/(cm <sup>2</sup> √min)]	$\rho$ [kΩcm]
28 days	1716.65 ± 11.80 (0.69%)	0.191 ± 0.018 (9.16%)	1.06 ± 0.04 (3.65%)	1847.66 ± 20.37 (1.10%)	0.094 ± 0.037 (39.48%)	1.44 ± 0.08 (5.81%)
180 days	1718.14 ± 9.21 (0.54%)	0.200 ± 0.012 (6.04%)	1.27 ± 0.06 (4.56%)	1830.52 ± 17.73 (0.97%)	0.147 ± 0.037 (25.40%)	1.57 ± 0.15 (9.75%)

<sup>1</sup> This table shows the average data with its standard deviation and, in brackets, the coefficient of variation.

Results confirm that finer-grained blocks absorb more water than coarser-grained ones. However, the results of the latter are more dispersed (Figure 12a). The results also show some correspondence with the electrical resistivity (Figure 12b).

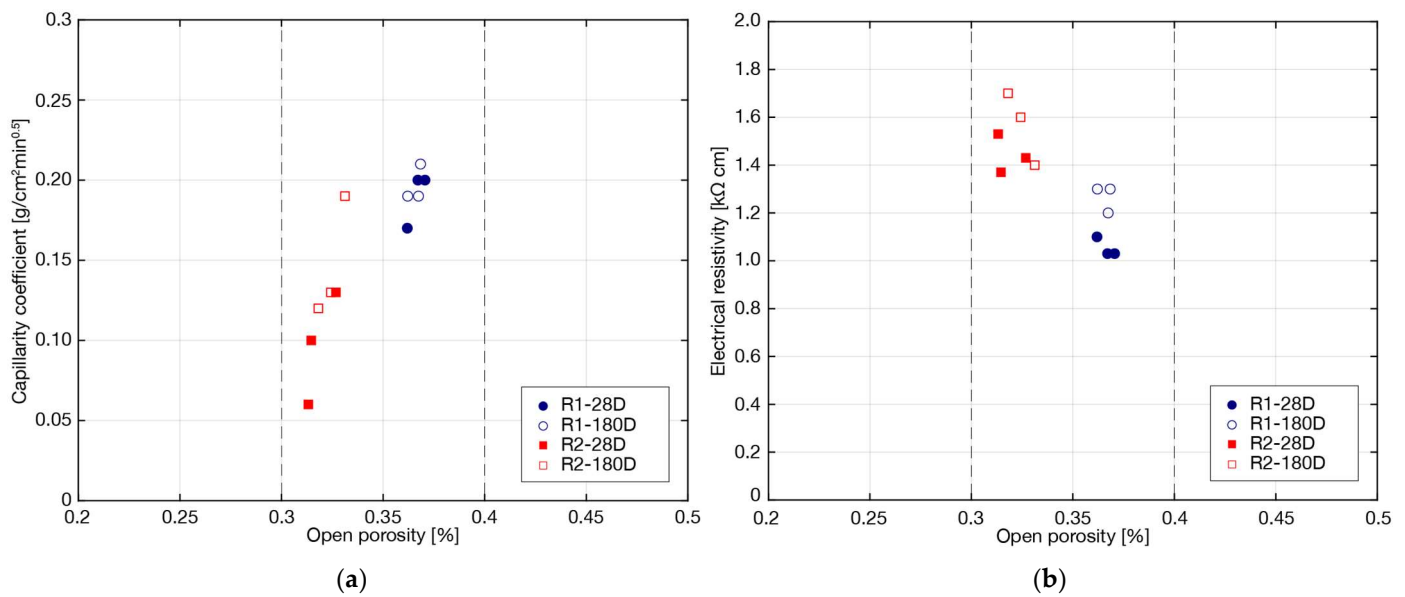


Figure 12. (a) Open porosity vs. capillarity coefficient; (b) Open porosity vs. electrical resistivity.

In porous media such as soil, the electrical resistivity can depend on factors such as the nature of the constituents, porous structure, degree of saturation, salt concentration and temperature [56]. In general, higher resistivity values indicate a lower electrical conductivity, which can be an indication of denser and more compacted material. In this study, besides the porous structure, the other listed variables can be neglected as they were kept constant. Therefore, the results obtained can be attributed to the effect of particle size.

### 3.6. Water Absorption by Total Immersion

During this test, although mass gain was measured at regular intervals, many blocks broke before an hour. This was due to the very small amount of stabiliser. In this regard, let us recall that only 5% by volume of hydraulic lime was used for stabilisation. After fifteen minutes, most of the blocks (of both ages) had, in fact, reached saturation and disintegrated. Some R1 blocks, cured for 180 days, withstood the 30- and 45-min measurements but could not be considered valid due to the large amount of mass lost. As a rule of thumb, according to the literature [57], samples disintegrate if more than 15% water is absorbed. For the sake of comparison, Table 10 reports the percentages of water absorbed after fifteen minutes of testing.

Table 10. Total water absorption test results <sup>1</sup>.

	R1 CEBs		R2 CEBs	
	$\gamma_d$ [kg/m <sup>3</sup> ]	$W_{15'}$ [%]	$\gamma_d$ [kg/m <sup>3</sup> ]	$W_{15'}$ [%]
28 days	1735.81 ± 5.18 (0.30%)	20.22 ± 1.83 (9.06%)	1890.74 ± 15.93 (0.84%)	15.34 ± 1.91 (12.45%)
180 days	1686.72 ± 33.42 (1.98%)	20.32 ± 6.53 (32.17%)	1837.39 ± 21.53 (1.17%)	15.70 ± 4.43 (28.25%)

<sup>1</sup> This table shows the average data with its standard deviation and, in brackets, the coefficient of variation.

The trend observed in the results is consistent between the two mixtures at both ages. In the first fifteen minutes, finer-textured R1 CEBs absorbed more water than coarse-textured R2 CEBs: 24.13% more at 28 days and 22.74% at 180 days (Figure 13). This observation emphasises the role of particle grading in the physical properties of CEBs.

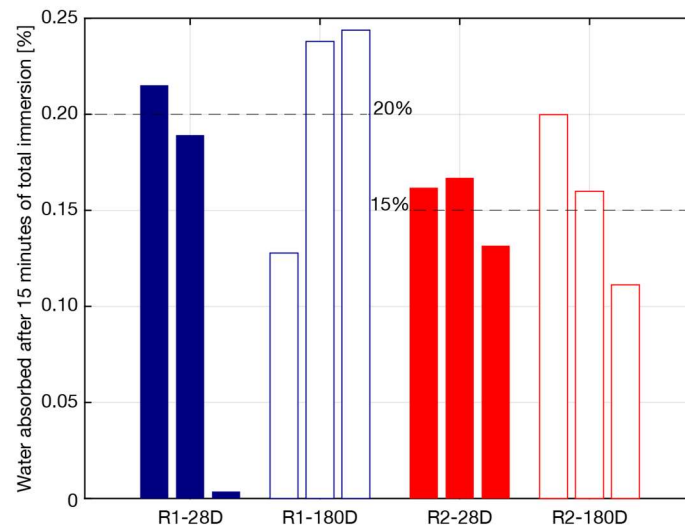


Figure 13. Water absorbed by total immersion after 15 min.

### 3.7. Erodibility Index

According to New Zealand’s Standard 4298 [35], erosion is the set of physical and chemical processes by which earthen construction materials wear away. It includes the processes of ageing and mechanical wear, simulated here through the pressure spray erosion test. The results of the test are summarised in Table 11.

Table 11. Spray erosion test results <sup>1</sup>.

	R1 CEBs			R2 CEBs		
	$\gamma$ [kg/m <sup>3</sup> ]	Rate of Erosion [mm/min]	Erodibility Index	$\gamma$ [kg/m <sup>3</sup> ]	Rate of Erosion [mm/min]	Erodibility Index
28 days	1717.65 ± 21.15 (1.23%)	5.18 ± 0.08 (1.54%)	5 (test failed)	1821.61 ± 9.49 (0.52%)	5.71 ± 0.10 (1.75%)	5 (test failed)

<sup>1</sup> This table shows the average data with its standard deviation and, in brackets, the coefficient of variation.

None of the mixtures passed the test. Although R1 CEBs exhibited a slightly lower erosion rate (10%), the results can still be considered comparable and were quite high. The pressure erosion test is considered by many to be an aggressive test that does not reproduce realistic atmospheric conditions [57]. However, according to [58], it can still be a good indicator of the material’s resistance to wind-driven rain. In this study, it did not provide usable results because the blocks were disintegrated by the water after only a few minutes (Figure 14). Therefore, it was decided not to repeat it at 180 days.



Figure 14. Condition of the blocks after spray erosion test.

### 3.8. Overview and Final Remarks

For ease of comparison, Table 12 provides an overview of the main physical, thermal, mechanical, and durability properties of the two batches of CEBs investigated in this study at the two ages of 28 and 180 days.

**Table 12.** Overview of the results obtained at 28 and 180 days.

ID	Physical			Thermal			Mechanical				Durability			
	$\gamma$	$\varphi$	$\omega$	R	$\lambda$	$\alpha$	$\sigma_c$	E	UPV <sub>30cm</sub>	$\sigma_f$	C <sub>b</sub>	$\rho$	W <sub>15'</sub>	D
R1-28D	1.72	36	1.40	0.30	0.50	$3.37 \times 10^{-7}$	2.54	55.65	1018.65	0.25	0.19	1.06	20	310.67
R2-28D	1.90	31	1.40	0.23	0.65	$4.04 \times 10^{-7}$	2.27	53.61	1004.57	0.21	0.09	1.44	15	342.67
R1-180D	1.73	37	0.79	0.30	0.50	$3.29 \times 10^{-7}$	1.78	40.46	974.71	0.25	0.20	1.27	20	-
R2-180D	1.85	32	0.60	0.23	0.65	$3.99 \times 10^{-7}$	2.03	46.21	1079.09	0.21	0.15	1.57	16	-

Units:  $\gamma$  [g/cm<sup>3</sup>]*—*bulk density;  $\varphi$  [%]*—*open porosity;  $\omega$  [%]*—*natural moisture content; R-value [m<sup>2</sup>K/W]*—*thermal resistance;  $\lambda$  [W/mK]*—*thermal conductivity;  $\alpha$  [m<sup>2</sup>/s]*—*thermal diffusivity;  $\sigma_c$  [MPa]*—*ultimate compressive strength; E-Modulus [MPa]; UPV<sub>30cm</sub> [m/s]*—*ultrasound pulse velocity;  $\sigma_f$  [MPa]*—*ultimate flexural strength; C<sub>b</sub> [g/(cm<sup>2</sup>√min)]*—*coefficient of capillarity absorption;  $\rho$  [kΩcm]*—*electrical resistivity; W<sub>15'</sub> [%]*—*water absorption by total immersion; D [mm/h]*—*rate of erosion.

In terms of physical attributes, blocks made from the finest soil (R1) have a lower bulk density than coarse-grained ones (R2), and the estimated open porosity was higher. In fact, these blocks absorbed more water during the water absorption tests, thus confirming the result. The natural moisture content at 28 days was not distinguishable between the two batches, which were probably still too humid. At 180 days, however, it was higher in the finer-textured blocks, which retain more water, as expected.

From the point of view of a building material, superior thermal properties were achieved in R1 blocks. Within the same volume, smaller soil particles have a larger surface area and more contact points, which inhibit heat transfer to a greater extent. Finer-textured R1 CEBs exhibited 23% higher thermal resistance, 30% lower thermal conductivity and 20% lower diffusivity than R2 CEBs. This result agrees with the literature that relates lower density with lower thermal conductivity [7,49]. However, strategies involving the addition or mixing of different materials in different proportions are usually used to vary the density [49,50]. In the case of this study, the variations obtained can only be attributed to the difference in maximum particle size. It would be interesting to confirm the results with other types of soil.

Regarding mechanical and durability properties, the results in the current literature are not confirmed. Blocks made from finer soil particles are not stronger or more durable [8–10]. However, results are not fully comparable as the mentioned studies either add sand or reconstitute the soil, leading to a substantial change in the natural state of the soil.

In the present study—that is, in the context of the same soil quality—the mechanical properties do not exhibit such an appreciable change due to the particle size effect. The data are scattered, but all fall within a similar range. At 28 days, R1 CEBs were slightly stronger than R2 CEBs (compressive strength 12% higher). In contrast, at 180 days, the compressive strength of R1 blocks was 14% lower than that of R2 blocks. The inverse relationship of physical attributes with mechanical strength was not verified.

The possibility of using UPV as a quick, non-destructive, and inexpensive tool to assess the quality of the blocks was also evaluated. At 28 days, the results obtained were not significantly different between the two mixtures. This might also be due to the higher moisture content. At 180 days, the ultrasonic pulse propagated faster in the denser R2 blocks, confirming the hypothesis of higher porosity in the R1 blocks. The UPV values showed no correspondence with mechanical parameters such as compressive strength or elastic modulus. Finally, at both ages, R1 CEBs showed slightly higher flexural strength than R2 CEBs. However, also considering the coefficients of variation, the results are superimposable.

The evaluation of durability aspects is based on three types of disintegrative mechanisms. It must be remembered that all existing test methods suffer from limitations related

to the nature of the material and may not reproduce actual conditions. Properly laid, sheltered, and plastered blocks—at least for exterior walls—are hardly exposed to extreme conditions such as water sprays or total immersion. However, for scientific purposes, it is of great interest to perform them. Beckett et al. [57] classified the capillary absorption test as a long-term durability that can be used to assess durability under non-extreme conditions. On the other hand, the total immersion and accelerated erosion tests are classified as short-term tests to assess the effectiveness of stabilisers and, more likely, extreme events rather than to predict the rate of erosion. Testing more than one disintegration mechanism allows not to draw approximate and/or erroneous conclusions about the resistance of the blocks to weathering [58].

In both water absorption tests, the finer-textured R1 blocks absorbed more water than the coarser-textured R2 ones. The water absorption coefficient by capillarity was 51% higher in R1 CEBs than R2 at 28 days and 26% higher in R1 CEBs than R2 at 180 days. After 15 min of soaking, R1 CEBs absorbed 24% more water than R2 at 28 days and 23% more water than R2 CEBs at 180 days.

Due to the low stabilisation rate, the accelerated erosion test did not produce interesting results. In fact, the blocks eroded at a very high rate in both mixtures and were completely disintegrated after only a few minutes. No mechanism could be identified, so the test was not repeated at 180 days.

#### 4. Conclusions

This study provides a comprehensive overview of the influence of soil particle size on the main properties of CEBs. Results show that particle size is a pivotal parameter with a significant influence on the problem examined, especially regarding the thermophysical attributes and water absorption capacity. Blocks made from finer soil (R1) exhibit lower bulk density and higher thermal resistance than blocks with a coarser texture. On the other hand, blocks made from coarser soil (R2) retain less water. No significant mechanical strength changes were observed. The results of this study open pathways for further research and practical applications in sustainable construction. Future studies should extend the main findings presented to verify whether these apply as a rule across different soil types. The relationship between moisture content and thermal attributes also requires further exploration to gain a comprehensive understanding of the magnitude of the effect. Confirmatory studies, in addition to providing new data to the literature, could help outline new and more sustainable strategies to optimise the properties of CEBs and the use of natural resources. Building on this research, future perspectives include the study of innovative techniques to improve the thermal performance of CEBs, such as incorporating additives or modifying production processes. Furthermore, the exploration of potential synergies between CEBs and other sustainable building materials could lead to the development of integrated solutions for environmentally friendly building practices. Overall, continued research in this area promises to advance the field of sustainable construction and address the most pressing challenges of the built environment.

**Author Contributions:** Conceptualization, C.T., A.P.J., E.T. and J.F.; methodology, C.T., A.P.J., E.T. and J.F.; investigation, C.T., A.P.J., C.J., E.T. and J.F.; data curation, C.T. and A.P.J.; writing—original draft preparation, C.T.; writing—review and editing, C.T., A.P.J., E.T., J.F. and R.M.; visualisation, C.T.; supervision, E.T., J.F. and R.M.; project administration, R.M.; funding acquisition, R.M. All authors have read and agreed to the published version of the manuscript.

**Funding:** This work was partly funded by Fundação “La Caixa” (Programa Promove) under the project BTCpro with the reference PV20-00072 and by FCT/MCTES through national funds (PID-DAC) under the R&D Unit Institute for Sustainability and Innovation in Structural Engineering (ISISE), reference UIDB/04029/2020 (doi.org/10.54499/UIDB/04029/2020), and under the Associate Laboratory Advanced Production and Intelligent Systems ARISE, reference LA/P/0112/2020. This work was also funded by national funds through FCT—Foundation for Science and Technology, under grant agreement UIDB/150874/2021, attributed to the first author, and under grant agreement

SFRH/BD/151345/2021, with funds from the European Social Fund (ESF) and Por Norte Program, under MIT Portugal Program, attributed to the second author.

**Institutional Review Board Statement:** Not applicable.

**Informed Consent Statement:** Not applicable.

**Data Availability Statement:** The raw data supporting the conclusions of this article will be made available by the authors on request.

**Conflicts of Interest:** The authors declare no conflicts of interest.

## References

1. Fernandes, J.; Peixoto, M.; Mateus, R.; Gervásio, H. Life cycle analysis of environmental impacts of earthen materials in the Portuguese context: Rammed earth and compressed earth blocks. *J. Clean. Prod.* **2019**, *241*, 118286. [CrossRef]
2. Schweiker, M.; Endres, E.; Gosslar, J.; Hack, N.; Hildebrand, L.; Creutz, M.; Klinge, A.; Kloft, H.; Knaack, U.; Mehnert, J.; et al. Ten questions concerning the potential of digital production and new technologies for contemporary earthen constructions. *Build. Environ.* **2021**, *206*, 108240. [CrossRef]
3. Ben-Alon, L.; Rempel, A.R. Thermal comfort and passive survivability in earthen buildings. *Build. Environ.* **2023**, *238*, 110339. [CrossRef]
4. Fabbri, A.; Aubert, J.-E.; Bras, A.A.; Faria, P.; Gallipoli, D.; Goffart, J.; McGregor, F.; Perlot-Bascoules, C.; Soudani, L. Hygrothermal and Acoustic Assessment of Earthen Materials. In *Testing and Characterisation of Earth-Based Building Materials and Elements*; Springer: Berlin/Heidelberg, Germany, 2022; pp. 83–126. [CrossRef]
5. Rigassi, V. *Compressed Earth Blocks: Manual of Production*; Deutsches Zentrum für Entwicklungstechnologien: Tübingen, Germany, 1985.
6. Fabbri, A.; Morel, J.C.; Aubert, J.-E.; Bui, Q.-B.; Gallipoli, D.; Ventura, A.; Reddy, V.B.V.; Hamard, E.; Pelé-Peltier, A.; Abhilash, H.N. An overview of the remaining challenges of the RILEM TC 274-TCE, testing and characterisation of earth-based building materials and elements. *RILEM Tech. Lett.* **2022**, *6*, 150–157. [CrossRef]
7. Mansour, M.B.; Jelidi, A.; Cherif, A.S.; Jabrallah, S.B. Optimizing thermal and mechanical performance of compressed earth blocks (CEB). *Constr. Build. Mater.* **2016**, *104*, 44–51. [CrossRef]
8. Cuccurullo, A.; Gallipoli, D.; Bruno, A.W.; Augarde, C.; Hughes, P.; La Borderie, C. Influence of particle grading on the hygromechanical properties of hypercompacted earth. *J. Build. Pathol. Rehabil.* **2020**, *5*, 2. [CrossRef]
9. Cuccurullo, A.; Gallipoli, D.; Bruno, A.W.; Augarde, C.; Hughes, P.; La Borderie, C. A comparative study of the effects of particle grading and compaction effort on the strength and stiffness of earth building materials at different humidity levels. *Constr. Build. Mater.* **2021**, *306*, 124770. [CrossRef]
10. Reddy, B.V.V.; Latha, M.S. Influence of soil grading on the characteristics of cement stabilised soil compacts. *Mater. Struct. Mater. Et. Constr.* **2013**, *47*, 1633–1645. [CrossRef]
11. Hall, M.; Allinson, D. Assessing the effects of soil grading on the moisture content-dependent thermal conductivity of stabilised rammed earth materials. *Appl. Therm. Eng.* **2009**, *29*, 740–747. [CrossRef]
12. Van Damme, H.; Houben, H. Earth concrete. Stabilization revisited. *Cem. Concr. Res.* **2018**, *114*, 90–102. [CrossRef]
13. Nagaraj, H.B.; Rajesh, A.; Sravan, M.V. Influence of soil gradation, proportion and combination of admixtures on the properties and durability of CSEBs. *Constr. Build. Mater.* **2016**, *110*, 135–144. [CrossRef]
14. Malkanthi, S.N.; Perera, A. Particle Packing Application for Improvement in the Properties of Compressed Stabilized Earth Blocks with Reduced Clay and Silt. *Eng. Technol. Appl. Sci. Res.* **2019**, *9*, 4538–4542. Available online: [www.etasr.com](http://www.etasr.com) (accessed on 4 August 2023). [CrossRef]
15. Malkanthi, S.N.; Wickramasinghe, W.G.S.; Perera, A. Use of construction waste to modify soil grading for compressed stabilized earth blocks (CSEB) production. *Case Stud. Constr. Mater.* **2021**, *15*, e00717. [CrossRef]
16. CRAterre-EAG. *Compressed Earth Blocks: Standards—Technology Series No.11*; CRAterre-EAG: Rome, Italy, 1998.
17. Delgado, M.C.J.; Guerrero, I.C. The selection of soils for unstabilised earth building: A normative review. *Constr. Build. Mater.* **2007**, *21*, 237–251. [CrossRef]
18. LNEC NP 143, *Solos*; Determinação dos Limites de Consistência—Soils. Determination of Consistency Limits. LNEC: Lisbon, Portugal, 1969. (In Portuguese)
19. LNEC NP-83, *Solos*; Determinação da Densidade das Partículas—Soils. Determination of Particle Density. LNEC: Lisbon, Portugal, 1965. (In Portuguese)
20. E1269-11; Standard Test Method for Determining Specific Heat Capacity by Differential Scanning Calorimetry. ASTM International: West Conshohocken, PA, USA, 2011.
21. LNEC E 197, *Solos*; Ensaio de Compactação—Soils. Compaction Test. LNEC: Lisbon, Portugal, 1966. (In Portuguese)
22. NP EN 933-8; Ensaio das Propriedades Geométricas dos Agregados: Parte 8: Determinação do Teor de Finos: Ensaio do Equivalente de Areia—Tests for Geometrical Properties of Aggregates: Part 8: Assessment of Fines: Sand Equivalent Test. Instituto Português da Qualidade: Caparica, Portugal, 2002. (In Portuguese)

23. NP EN 933-9; Ensaios das Propriedades Geométricas dos Agregados: Parte 9: Determinação do Teor de Finos: Ensaio do Azul de Metileno—Tests for Geometrical Properties of Aggregates: Part 9: Assessment of Fines: Methylene Blue Test. Instituto Português da Qualidade: Caparica, Portugal, 2002. (In Portuguese)
24. ASTM D 2974; Standard Test Methods for Moisture, Ash, and Organic Matter of Peat and Other Organic Soils. ASTM International: West Conshohocken, PA, USA, 2014.
25. Minke, G. *Building with Earth: Design and Technology of a Sustainable Architecture*; Walter de Gruyter GmbH: Berlin, Germany, 2009. [[CrossRef](#)]
26. ASTM C1363; 11 Standard Test Method for Thermal Performance of Building Materials and Envelope Assemblies by Means of a Hot Box Apparatus 1. American Society for Testing Materials 90: West Conshohocken, PA, USA, 2014.
27. ISO 9869-1:2014; Thermal Insulation—Building Elements—Insitu Measurement of Thermal Resistance and Thermal Transmittance; Part 1: Heat Flow Meter Method. BSI: London, UK, 2014.
28. Teixeira, E.R.; Machado, G.; De Adilson, P.; Guarnier, C.; Fernandes, J.; Silva, S.M.; Mateus, R. Mechanical and thermal performance characterisation of compressed earth blocks. *Energies* **2020**, *13*, 2978. [[CrossRef](#)]
29. NP EN 772-1; Método de Ensaio de Blocos Para Alvenaria. Parte 1: Determinação da Resistência à Compressão—Methods of Test for Masonry Units. Part 1: Determination of Compressive Strength. Instituto Português da Qualidade: Caparica, Portugal, 2002. (In Portuguese)
30. NP EN 12504-4; Ensaios do Betão nas Estruturas. Parte 4: Determinação da Velocidade de Propagação dos Ultra-Sons—Testing Concrete in Structures. Part 4: Determination of Ultrasonic Pulse Velocity. Instituto Português da Qualidade: Caparica, Portugal, 2007. (In Portuguese)
31. Carrasco, E.V.M.; Silva, S.R.; Mantilla, J.N.R. Assessment of Mechanical Properties and the Influence of the Addition of Sawdust in Soil–Cement Bricks Using the Technique of Ultrasonic Anisotropic Inspection. *J. Mater. Civ. Eng.* **2014**, *26*, 219–225. [[CrossRef](#)]
32. Kasinikota, P.; Tripura, D.D. Prediction of physical-mechanical properties of hollow interlocking compressed unstabilized and stabilized earth blocks at different moisture conditions using ultrasonic pulse velocity. *J. Build. Eng.* **2022**, *48*, 103961. [[CrossRef](#)]
33. LNEC E 393, *Betões*; Determinação da Absorção de Água por Capilaridade—Concrete. Determination of the Absorption of Water through Capillarity. LNEC: Lisbon, Portugal, 1993. (In Portuguese)
34. LNEC E 394, *Betões*; Determinação da Absorção de Água por Imersão—Concrete. Determination of the Absorption of Water by Immersion. LNEC: Lisbon, Portugal, 1993. (In Portuguese)
35. NZS 4298; Materials and Workmanship for Earth Buildings. Standards New Zealand: Wellington, New Zealand, 1998.
36. Zheng, J.; Carlson, W.B.; Reed, J.S. The packing density of binary powder mixtures. *J. Eur. Ceram. Soc.* **1995**, *15*, 479–483. [[CrossRef](#)]
37. Kwan, A.K.H.; Chan, K.W.; Wong, V. A 3-parameter particle packing model incorporating the wedging effect. *Powder Technol.* **2013**, *237*, 172–179. [[CrossRef](#)]
38. Zhang, N.; Yu, X.; Pradhan, A.; Puppala, A.J. Effects of Particle Size and Fines Content on Thermal Conductivity of Quartz Sands. *Transp. Res. Rec.* **2015**, *2510*, 36–43. [[CrossRef](#)]
39. Moevus, M.; Anger, R.; Fontaine, L. Hygro-Thermo-Mechanical Properties of Earthen Materials for Construction: A Literature Review. In Proceedings of the Terra 2012, XIth International Conference on the Study and Conservation of Earthen Architectural Heritage, Lima, Peru, 22–27 April 2012; pp. 1–10.
40. Gemant, A. The thermal conductivity of soils. *J. Appl. Phys.* **1950**, *21*, 750–752. [[CrossRef](#)]
41. Ochsner, T. *Rain or Shine: An Introduction to Soil Physical Properties and Processes*; Oklahoma State University Library: Stillwater, OK, USA, 2019. [[CrossRef](#)]
42. He, H.; He, Y.; Cai, G.; Wang, Y.; Zhang, G. Influence of particle size and packing on the thermal conductivity of carbonate sand. *Granul. Matter* **2022**, *24*, 117. [[CrossRef](#)]
43. Persson, B.N.J. Heat transfer in granular media consisting of particles in humid air at low confining pressure. *Eur. Phys. J. B* **2023**, *96*, 14. [[CrossRef](#)]
44. Midttømme, K.; Roaldset, E. The effect of grain size on thermal conductivity of quartz sands and silts. *Pet. Geosci.* **1998**, *4*, 165–172. [[CrossRef](#)]
45. Boulmaali, M.; Belhamri, A. Investigation of thermal inertia and hydric properties of an eco-building material: Compressed stabilized earth blocks. *Heat. Mass. Transf.* **2023**, *59*, 713–727. [[CrossRef](#)]
46. Zhang, L.; Gustavsen, A.; Jelle, B.P.; Yang, L.; Gao, T.; Wang, Y. Thermal conductivity of cement stabilized earth blocks. *Constr. Build. Mater.* **2017**, *151*, 504–511. [[CrossRef](#)]
47. Bruno, A.W.; Gallipoli, D.; Perlot, C.; Kallel, H. Thermal performance of fired and unfired earth bricks walls. *J. Build. Eng.* **2020**, *28*, 101017. [[CrossRef](#)]
48. Adam, E.A.; Jones, P.J. Thermophysical properties of stabilised soil building blocks. *Build. Env.* **1995**, *30*, 245–253. [[CrossRef](#)]
49. Turco, C.; Junior, A.C.P.; Teixeira, E.; Mateus, R. Optimisation of Compressed Earth Blocks (CEBs) using natural origin materials: A systematic literature review. *Constr. Build. Mater.* **2021**, *309*, 125140. [[CrossRef](#)]
50. Turco, C.; de Paula Junior, A.; Teixeira, E.; Mateus, R. Authors closure to the Discussion of the Review article “Optimisation of Compressed earth blocks (CEBs) using natural origin materials: A systematic literature review”. *Constr. Build. Mater.* **2022**, *325*, 126888. [[CrossRef](#)]

51. Fabbri, A.; Morel, J.C.; Aubert, J.E.; Bui, Q.B.; Gallipoli, D.; Reddy, B.V.V. *Testing and Characterisation of Earth-Based Building Materials and Elements: State-of-the-Art Report of the RILEM TC 274-TCE*; Springer: Berlin/Heidelberg, Germany, 2022.
52. Atiki, E.; Taallah, B.; Feia, S.; Almeasar, K.S.; Guettala, A. Effects of Incorporating Date Palm Waste as a Thermal Insulating Material on the Physical Properties and Mechanical Behavior of Compressed Earth Block. *J. Nat. Fibers* **2022**, *19*, 8778–8795. [[CrossRef](#)]
53. Galán-Marín, C.; Rivera-Gómez, C.; Bradley, F. Ultrasonic, molecular and mechanical testing diagnostics in natural fibre reinforced, polymer-stabilized earth blocks. *Int. J. Polym. Sci.* **2013**, *2013*, 130582. [[CrossRef](#)]
54. Idder, A.; Hamouine, A.; Labbaci, B.; Abdeldjebar, R. The porosity of stabilized earth blocks with the addition plant fibers of the date palm. *Civ. Eng. J.* **2020**, *6*, 478–494. [[CrossRef](#)]
55. Sturm, T.; Ramos, L.F.; Lourenço, P.B. Characterization of dry-stack interlocking compressed earth blocks. *Mater. Struct./Mater. Et. Constr.* **2015**, *48*, 3059–3074. [[CrossRef](#)]
56. Samouëlian, A.; Cousin, I.; Tabbagh, A.; Bruand, A.; Richard, G. Electrical resistivity survey in soil science: A review. *Soil. Tillage Res.* **2005**, *83*, 173–193. [[CrossRef](#)]
57. Beckett, C.T.S.; Jaquin, P.A.; Morel, J.C. Weathering the storm: A framework to assess the resistance of earthen structures to water damage. *Constr. Build. Mater.* **2020**, *242*, 118098. [[CrossRef](#)]
58. Panagiotou, R.; Kyriakides, M.A.A.; Illampas, R.; Ioannou, I. An experimental approach for the investigation of the performance of non-stabilized Compressed Earth Blocks (CEBs) against water-mediated weathering. *J. Cult. Herit.* **2022**, *57*, 184–193. [[CrossRef](#)]

**Disclaimer/Publisher’s Note:** The statements, opinions and data contained in all publications are solely those of the individual author(s) and contributor(s) and not of MDPI and/or the editor(s). MDPI and/or the editor(s) disclaim responsibility for any injury to people or property resulting from any ideas, methods, instructions or products referred to in the content.